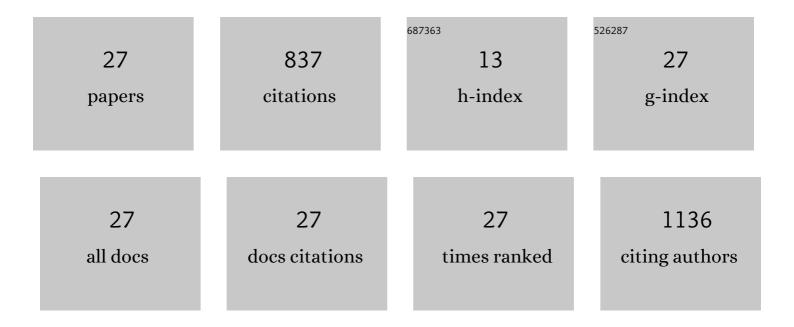
## **Tiandu Sheng**

List of Publications by Year in descending order

Source: https://exaly.com/author-pdf/1317716/publications.pdf Version: 2024-02-01



TIANDU SHENC

#	Article	IF	CITATIONS
1	Tetraethylenepentamine modified magnetic cellulose nanocrystal composites for removal of Congo red with high adsorption capacity. Journal of Dispersion Science and Technology, 2022, 43, 1858-1871.	2.4	7
2	Lattice Boltzmann phase field simulations of droplet slicing. Canadian Journal of Chemical Engineering, 2022, 100, .	1.7	1
3	Preparation and adsorbability of magnetic composites based on cellulose nanofiber/graphene oxide. Colloids and Surfaces A: Physicochemical and Engineering Aspects, 2022, 639, 128373.	4.7	14
4	Effect of Additives on Preferential Crystallization for the Chiral Resolution of Citrulline: Experimental, Statistical, and Molecular Dynamics Simulation Studies. Crystal Growth and Design, 2022, 22, 2392-2406.	3.0	11
5	Magnetically recyclable core–shell MOF nanoparticles of Fe <sub>3</sub> O <sub>4</sub> @PDA@UIO-66-NH <sub>2</sub> grafted by organic acids for intensified cationic dye adsorption. New Journal of Chemistry, 2022, 46, 11071-11081.	2.8	21
6	Direct Crystallization Resolution of Racemates Enhanced by Chiral Nanorods: Experimental, Statistical, and Quantum Mechanics/Molecular Dynamics Simulation Studies. ACS Omega, 2022, 7, 19828-19841.	3.5	6
7	Using Amphiphilic Polymer Micelles as the Templates of Antisolvent Crystallization to Produce Drug Nanocrystals. ACS Omega, 2022, 7, 21000-21013.	3.5	5
8	Doubly modified MWCNTs embedded in polyethersulfone (PES) ultrafiltration membrane and its anti-fouling performance. Journal of Polymer Engineering, 2022, 42, 885-898.	1.4	3
9	Preparation of a PES/PFSA- <i>g</i> -MWCNT ultrafiltration membrane with improved permeation and antifouling properties. New Journal of Chemistry, 2021, 45, 4950-4962.	2.8	6
10	A graphene oxide modified cellulose nanocrystal/PNIPAAm IPN hydrogel for the adsorption of Congo red and methylene blue. New Journal of Chemistry, 2021, 45, 16679-16688.	2.8	12
11	A novel PVDF/PFSA-g-GO ultrafiltration membrane with enhanced permeation and antifouling performances. Separation and Purification Technology, 2020, 233, 116038.	7.9	66
12	Experimental and Molecular Dynamics Simulation Study on the Primary Nucleation of Penicillamine Racemate and Its Enantiomers in the Mixture Solvent of Water and Ethanol. Industrial & Engineering Chemistry Research, 2020, 59, 21957-21968.	3.7	13
13	The construction of CuCo <sub>2</sub> O <sub>4</sub> /N-doped reduced graphene oxide hybrid hollow spheres as anodes for sodium-ion batteries. New Journal of Chemistry, 2020, 44, 6739-6746.	2.8	10
14	Triethylenetetramine-modified hollow Fe3O4/SiO2/chitosan magnetic nanocomposites for removal of Cr(VI) ions with high adsorption capacity and rapid rate. Microporous and Mesoporous Materials, 2020, 297, 110041.	4.4	74
15	Self-Assembly of Emissive Nanocellulose/Quantum Dot Nanostructures for Chiral Fluorescent Materials. ACS Nano, 2019, 13, 9074-9081.	14.6	115
16	Facile construction of dual functional Fe3O4@C-MoO2-Ni composites for catalysis and adsorption. Applied Surface Science, 2019, 494, 783-794.	6.1	27
17	Molecular Simulation Approaches for the Prediction of Unknown Crystal Structures and Solubilities of ( <i>R</i> )- and ( <i>R</i> , <i>S</i> )-Crizotinib in Organic Solvents. Crystal Growth and Design, 2019, 19, 5882-5895.	3.0	17
18	Amperometric sensor for dopamine based on surface-graphenization pencil graphite electrode prepared by in-situ electrochemical delamination. Mikrochimica Acta, 2019, 186, 324.	5.0	18

TIANDU SHENG

#	Article	IF	CITATIONS
19	Wrapping Nanocellulose Nets around Graphene Oxide Sheets. Angewandte Chemie - International Edition, 2018, 57, 8508-8513.	13.8	93
20	Fabrication of xanthate-modified chitosan/poly(N-isopropylacrylamide) composite hydrogel for the selective adsorption of Cu(II), Pb(II) and Ni(II) metal ions. Chemical Engineering Research and Design, 2018, 139, 197-210.	5.6	71
21	Facile assembling of novel polypyrrole nanocomposites theranostic agent for magnetic resonance and computed tomography imaging guided efficient photothermal ablation of tumors. Journal of Colloid and Interface Science, 2018, 530, 547-555.	9.4	32
22	Facile fabrication of a magnetically smart PTX-loaded Cys–Fe <sub>3</sub> O <sub>4</sub> /CuS@BSA nano-drug for imaging-guided chemo-photothermal therapy. Dalton Transactions, 2017, 46, 2204-2213.	3.3	18
23	Fe 3 O 4 @SiO 2 @CS-TETA functionalized graphene oxide for the adsorption of methylene blue (MB) and Cu(II). Applied Surface Science, 2017, 420, 970-981.	6.1	147
24	Facile one-pot synthesis of Fe <sub>3</sub> O <sub>4</sub> @chitosan nanospheres for MRI and fluorescence imaging guided chemo-photothermal combinational cancer therapy. Dalton Transactions, 2016, 45, 19519-19528.	3.3	27
25	Solubility Measurement and Simulation of Rivaroxaban (Form I) in Solvent Mixtures from 273.15 to 323.15 K. Journal of Chemical & Engineering Data, 2016, 61, 495-503.	1.9	9
26	Synthesis of Amine-Terminated Polyether over Cobalt Catalyst: Influence of Reaction Parameters. Materials and Manufacturing Processes, 2014, 29, 738-742.	4.7	3
97	Solubility of Two Polymorphs of Erlotinib Hydrochloride in Isopropanol and Acetone from (273.15 to) Tj ETQq1 1	0.784314	rgBT /Overl